1-1-2019

# Multiple Aneurysms AnaTomy CHallenge 2018 (MATCH)—Phase II: rupture risk assessment

Philipp Berg
*Otto von Guericke University Magdeburg*

Samuel Voß
*Simula Research Laboratory*

Gábor Janiga
*Charité Universitätsmedizin Berlin*

Sylvia Saalfeld
*Helios Hospital Berlin Buch*

Aslak W. Bergersen
*University of Hong Kong*

International Journal of Computer Assisted Radiology and Surgery (2019) 14:1795–1804
https://doi.org/10.1007/s11548-019-01986-2

ORIGINAL ARTICLE

# Multiple Aneurysms AnaTomy CHallenge 2018 (MATCH)—phase II: rupture risk assessment

**Philipp Berg[1] · Samuel Voß[1] · Gábor Janiga[1] · Sylvia Saalfeld[1] · Aslak W. Bergersen[2] · Kristian Valen-Sendstad[2] · Jan Bruening[3] · Leonid Goubergrits[3] · Andreas Spuler[4] · Tin Lok Chiu[5] · Anderson Chun On Tsang[5] · Gabriele Copelli[6] · Benjamin Csippa[7] · György Paál[7] · Gábor Závodszky[7] · Felicitas J. Detmer[8] · Bong J. Chung[8] · Juan R. Cebral[8] · Soichiro Fujimura[9] · Hiroyuki Takao[9] · Christof Karmonik[10] · Saba Elias[10] · Nicole M. Cancelliere[11] · Mehdi Najafi[12] · David A. Steinman[12] · Vitor M. Pereira[11] · Senol Piskin[13] · Ender A. Finol[13] · Mariya Pravdivtseva[14] · Prasanth Velvaluri[15] · Hamidreza Rajabzadeh-Oghaz[16] · Nikhil Paliwal[16] · Hui Meng[16] · Santhosh Seshadhri[17] · Sreenivas Venguru[17] · Masaaki Shojima[18] · Sergey Sindeev[19] · Sergey Frolov[19] · Yi Qian[20] · Yu-An Wu[21] · Kent D. Carlson[21] · David F. Kallmes[21] · Dan Dragomir-Daescu[21] · Oliver Beuing[22]**

Received: 10 January 2019 / Accepted: 23 April 2019 / Published online: 3 May 2019


## Abstract

**Purpose** Assessing the rupture probability of intracranial aneurysms (IAs) remains challenging. Therefore, hemodynamic simulations are increasingly applied toward supporting physicians during treatment planning. However, due to several assumptions, the clinical acceptance of these methods remains limited.

**Methods** To provide an overview of state-of-the-art blood flow simulation capabilities, the Multiple Aneurysms AnaTomy CHallenge 2018 (MATCH) was conducted. Seventeen research groups from all over the world performed segmentations and hemodynamic simulations to identify the ruptured aneurysm in a patient harboring five IAs. Although simulation setups revealed good similarity, clear differences exist with respect to the analysis of aneurysm shape and blood flow results. Most groups (12/71%) included morphological and hemodynamic parameters in their analysis, with aspect ratio and wall shear stress as the most popular candidates, respectively.

**Results** The majority of groups (7/41%) selected the largest aneurysm as being the ruptured one. Four (24%) of the participating groups were able to correctly select the ruptured aneurysm, while three groups (18%) ranked the ruptured aneurysm as the second most probable. Successful selections were based on the integration of clinically relevant information such as the aneurysm site, as well as advanced rupture probability models considering multiple parameters. Additionally, flow characteristics such as the quantification of inflow jets and the identification of multiple vortices led to correct predictions.

**Conclusions** MATCH compares state-of-the-art image-based blood flow simulation approaches to assess the rupture risk of IAs. Furthermore, this challenge highlights the importance of multivariate analyses by combining clinically relevant metadata with advanced morphological and hemodynamic quantification.

**Keywords** Intracranial aneurysm · Rupture risk · Hemodynamic simulation · International challenge

✉ Philipp Berg
berg@ovgu.de

1 University of Magdeburg, Magdeburg, Germany
2 Simula Research Laboratory, Lysaker, Norway
3 Charité – Universitätsmedizin, Berlin, Germany
4 Helios Hospital Berlin Buch, Berlin, Germany
5 University of Hong Kong, Hong Kong, China
6 University of Parma, Parma, Italy
7 Budapest University of Technology and Economics, Budapest, Hungary
8 George Mason University, Fairfax, VA, USA
9 Tokyo University of Science, Tokyo, Japan
10 Houston Methodist Research Institute, Houston, TX, USA
11 Toronto Western Hospital, Toronto, ON, Canada

## Introduction

The assessment of intracranial aneurysm (IA) rupture probability or the differentiation between stable and unstable IAs still remains challenging. Hence, image-based hemodynamic simulations are increasingly used to account for patient-specific flow structures and detect potentially harmful conditions. However, the usefulness of computational fluid dynamics (CFD) in a clinical context remains uncertain.

After early single-case applications of numerical methods for IA flow description [1, 2], more advanced simulation studies containing larger case numbers were performed. Xiang et al. [3, 4] investigated 119 (and later 204) aneurysms using CFD and found that most ruptured IAs had complex flow, significantly lower wall shear stress (WSS), and larger oscillatory shear compared to the unruptured cohort. In contrast, Cebral et al. [5, 6] concluded (based on 210 cases) that rupture more likely occurs in IAs with significantly higher maximum WSS, concentrated inflow, and complex flow patterns. Recently, Detmer et al. [7] included 1631 aneurysms in their study and developed an aneurysm rupture probability model based on patient characteristics (age and gender), aneurysm location, morphology, and hemodynamics.

In addition to numerical investigations of blood flow, several verification and validation studies have been carried out to improve the acceptance of the underlying methods among physicians [8–12]. However, reliable acquisition of potentially relevant parameters can be difficult or be subject to a high variability, due to multiple interdisciplinary working steps. To address this observation and draw attention to required conditions for realistic hemodynamic simulations, Steinman et al. [13] organized a broad challenge (25 groups participating) that compared the fluid dynamics solver, discretization approaches, and solution strategies employed among participants. Good agreement with respect to cycle-average velocity and peak systolic pressure calculation was obtained, but other clinically relevant parameters were not addressed. In a follow-up challenge (26 groups participating) organized by Janiga and Berg, participants were requested to predict aneurysm rupture and the corresponding rupture site using numerical methods [14, 15]. Over 80% of the groups chose the correct aneurysm, but the rupture site could not be found based on CFD. To address the overall variability of the important hemodynamic parameter WSS, Valen-Sendstad et al. [16] compared simulation results from 28 challenge contributions, providing only the source 3D images to each team. Based on the normalized WSS results of five middle cerebral artery aneurysms per group, they found that the inter-group variability was around 30%, with the highest differences with respect to maximum WSS and low shear area.

The present study focuses on the presentation of state-of-the-art segmentation and simulation approaches with respect to IA rupture risk assessment. In the frame of the Multiple Aneurysms AnaTomy CHallenge 2018 (MATCH), interested biomedical engineering groups were requested to segment and simulate a patient-specific dataset harboring five IAs. Furthermore, rupture probability suggestions were collected based on arbitrary criteria (e.g., any number of morphological and/or hemodynamic parameters). The results of the first phase (segmentation) are presented in Berg et al. [17], while this study focuses on the second phase (rupture risk assessment). Based on the presented findings, helpful recommendations regarding realistic and beneficial blood flow simulations are provided for future investigations.

## Materials and methods

### Case details and image acquisition

All five aneurysms that were the subject of MATCH were found in a single patient admitted to the hospital with acute subarachnoid hemorrhage due to rupture of one of the aneurysms. Two aneurysms were located at the right M1-segment, one at the left M1-segment, another one at the left MCA-bifurcation, and the fifth at the left posterior inferior cerebellar artery (PICA) (see Fig. 1). Four aneurysms were of similar size ranging between 4.4 mm and 5.6 mm. The two M1-aneurysms on the right were clipped, the others coiled.

The ruptured aneurysm was clearly identified by imaging. CT and subsequent MRI showed a subarachnoid hemorrhage mainly in the left premedullary cistern surrounding the PICA-aneurysm. In addition, both M1-aneurysms on the right were clipped, with no evidence of prior bleeding. This study was performed in accordance with the guidelines of the local ethics committee.

[12] University of Toronto, Toronto, ON, Canada

[13] The University of Texas at San Antonio, San Antonio, TX, USA

[14] University Medical Center Schleswig-Holstein, Kiel, Germany

[15] Christian-Albrechts-University, Kiel, Germany

[16] State University of New York, Buffalo, NY, USA

[17] Medtronic Engineering Innovation Centre, Hyderabad, India

[18] Saitama Medical University General Hospital, Saitama, Japan

[19] Tambov State Technical University, Tambov, Russia

[20] Macquarie University, Sydney, Australia

[21] Mayo Clinic, Rochester, MN, USA

[22] University Hospital Magdeburg, Magdeburg, Germany

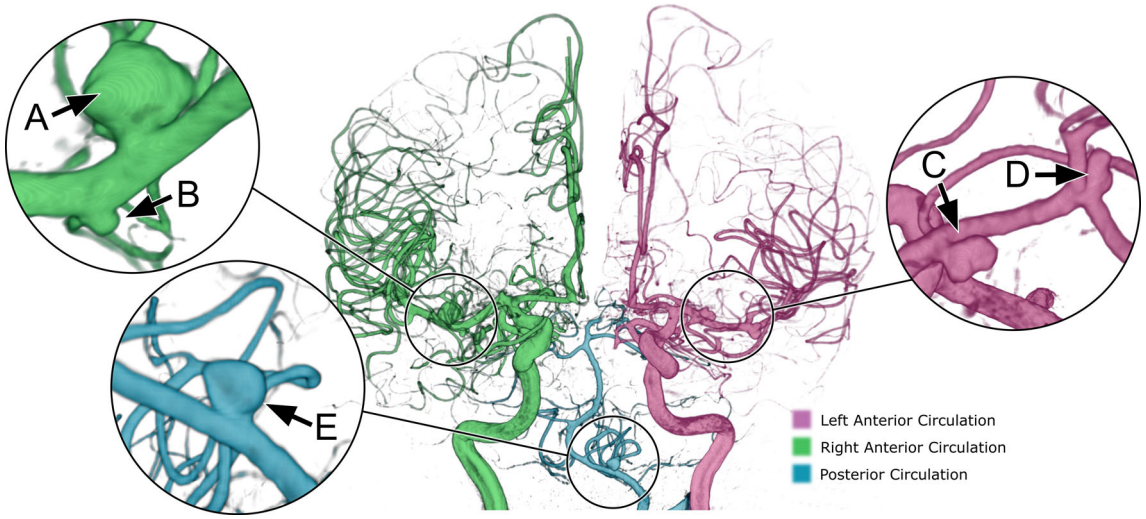


**Fig. 1** Illustration of the five IAs from the investigated aneurysm patient. Aneurysms A and B were located on the M1 segment of the right anterior circulation and C on the left M1 segment, respectively. Aneurysm D was found on the left middle cerebral artery bifurcation and aneurysm E was located on the left posterior inferior cerebellar artery. The image data were acquired using 2D and 3D digital subtraction angiography, while only 3D rotational angiography data were provided to the MATCH participants

## Participating groups

MATCH was initially announced on November 03, 2017, and interested research groups were able to receive detailed information from the associated Web site (https://www.ics2018.de) and from newsletters of the 15th Interdisciplinary Cerebrovascular Symposium. Participants were asked to submit their simulation results until February 02, 2018, wherein the following items were requested:

- Participants were asked to perform hemodynamic simulations based on their own segmentations, and to identify which aneurysm ruptured using arbitrary criteria (e.g., hemodynamic parameters). In addition to the request to decide which aneurysm ruptured, participants were asked to provide a rupture probability ranking of the five IAs.
- Participants submitted an informal abstract (max. 1 page) containing author names, affiliations, and simulation details: (1) Mesh resolution, (2) solver, (3) time-step size (if unsteady), (4) type of in- and outflow boundary condition, (5) viscosity/density, and (6) reasons for choosing a particular aneurysm as being the ruptured one (aneurysm A-E) as well as ranking of rupture probability of each aneurysm. Further details were optional.

In total, 17 groups from 11 different countries followed the call and submitted an abstract. The groups had the following origins: Europe (Germany: 2; Hungary, Italy, Norway, Russia: 1); North America (USA: 5; CAN: 1); Asia (Japan: 2; India, Hong Kong: 1); Australia (1).

## Segmentations

3D rotational angiographies acquired on an Artis Q angiography system (Siemens Healthineers AG, Forchheim, Germany) were reconstructed on a Syngo X Workplace (Siemens Healthineers AG, Forchheim, Germany) using the kernel "HU auto" [18]. The details of the segmentation have already been described in Berg et al. [17].

## Hemodynamic simulations

Since each participant had the freedom to choose an arbitrary strategy regarding the hemodynamic simulations, the most important properties are described in the following. An overview regarding the simulation setups for MATCH is presented in Table 1 and Fig. 2.

### Spatial discretization

Although a variety of meshing strategies related to CFD exists, the use of unstructured grids with a combination of either tetrahedral (14 groups) or polyhedral (2 groups) cells with a few prism layers was most common. Only one group used an unstructured hexahedral mesh with five additional prism layers (Group 2). Regardless of the mesh type, an appropriate spatial resolution is essential to enable the generation of mesh-independent solutions. Here, reported cell sizes ranged between 0.1 and 0.3 mm, with a mean value and standard deviation of $0.17 \pm 0.076$ mm. Thus, depending on the size of the considered vessel volume, the total number of cells per simulation was between 0.5 and 4.1 million.

**Table 1** Each group's technical details regarding the corresponding hemodynamic simulation and analysis as well as individual selections of the aneurysm with the highest rupture probability (correct choices are highlighted as bold)

| Group | Inlet boundary condition | Blood treatment | Time dependency | Outlet boundary condition | Time step size | Parameters | No. param. | Aneurysm choice |
|---|---|---|---|---|---|---|---|---|
| **1** | **Womersley** | **Newtonian** | **Unsteady** | **Zero pressure** | **1E−02** | **Morph/hemo** | **16** | **E** |
| 2 | Plug | Non-Newt. | Unsteady | Zero pressure | 1E−03 | Morph/hemo | 4 | A |
| 3 | Plug | Newtonian | Steady | Zero pressure | – | Morph/hemo | 2 | C |
| 4 | Plug | Newtonian | Steady | Murray (d2) | – | Hemo | 1 | D |
| 5 | Womersley | Newtonian | Unsteady | 0D model | 1E−04 | Morph/hemo | 6 | A |
| **6** | **2D PC-MRI** | **Non-Newt.** | **Unsteady** | **Constant pressure** | **1E−02** | **Morph/hemo** | **3** | **E** |
| 7 | Plug | Non-Newt. | Steady | Murray (d2) | – | Morph/hemo | 4 | A |
| **8** | **Womersley** | **Newtonian** | **Unsteady** | **Zero pressure** | **1E−03** | **Morph/hemo** | **4** | **E** |
| 9 | Womersley | Newtonian | Unsteady | 0D model | 1E−04 | Morph/hemo | 2 | D |
| 10 | Plug | Newtonian | Unsteady | Zero pressure | 5E−07 | Hemo | 2 | D |
| 11 | Parabolic | Newtonian | Steady | Murray (d3) | – | Morph/hemo | 2 | A |
| 12 | Plug | Newtonian | Unsteady | Pressure waveform | 5E−03 | Hemo | 3 | C |
| 13 | Plug | Newtonian | Unsteady | Murray (d2) | 1E−03 | Morph/hemo | 3 | C |
| 14 | Plug | Newtonian | Unsteady | Zero pressure | 5E−04 | Morph/hemo | 4 | A |
| **15** | **Parabolic** | **Newtonian** | **Unsteady** | **Zero pressure** | **7E−03** | **Hemo** | **5** | **E** |
| 16 | Plug | Newtonian | Steady | Zero pressure | – | Hemo | 5 | C |
| 17 | Plug | Newtonian | Unsteady | Pressure waveform | 1E−03 | Morph/hemo | 6 | A |

The following criteria are presented: (1) type of inlet boundary condition: constant (plug), parabolic, Womersley or phase-contrast magnetic resonance imaging (PC-MRI) profile, (2) blood treatment, assuming Newtonian or Non-Newtonian behavior, (3) time dependency: steady-state or time-varying simulations, (4) type of parameters for rupture risk assessment: morphologic and/or hemodynamic, (5) number of considered parameters, (6) selected aneurysm with the highest rupture probability

### Solver selection

To solve the equation for mass and momentum conservation, an appropriate and validated fluid dynamics solver is required. Here, most groups (11) decided to use a commercially available software package, which was either from ANSYS (Fluent or CFX, Canonsburg, Pennsylvania, USA) or from Siemens PLM (STAR CCM + , Plano, Texas, USA). Approximately one-third of the participants (five groups) applied open-source tools (e.g., OpenFOAM or Oasis). Only one group used an in-house fluid dynamics solver.

### Boundary conditions

Since only the image data were provided to the MATCH participants, patient-specific boundary conditions were not available. This represents a situation commonly encountered by research groups; as for the patient in this study with a subarachnoid hemorrhage, the acquisition of individual flow curves would mean an additional, unrequired intervention. Hence, participants were free to choose arbitrary boundary conditions.

Regarding the resolution of temporal effects, five groups (29%) performed steady-state simulations, while twelve groups (71%) considered unsteady flow with the simulation of two or more cardiac cycles. Interestingly, clear differences with respect to the time step size occurred, which ranged between 5E−7 s and 1E−2 s (mean 3E−3 ± 3.9E−3 s). Furthermore, variability regarding the type of inflow boundary condition was present. While 60% of the groups applied a constant plug profile for either velocity or flow rate, one quarter defined a *Womersley* equation profile, which describes the pulsatile character of the velocity profile. A parabolic flow was assumed by two groups and one group applied velocity profiles of the left internal carotid and vertebral artery from 2D phase-contrast MRI measurements of a healthy volunteer.

To characterize the entire computational system, outlet boundary conditions needed to be defined. Due to the lack of knowledge regarding pressure distributions in the distal vessels, eleven groups (65%) used either constant values or predefined pressure waves. The remaining six groups applied flow-splitting models, which were either based on in-house 0D models (two groups) [19], area-dependent weighting (two

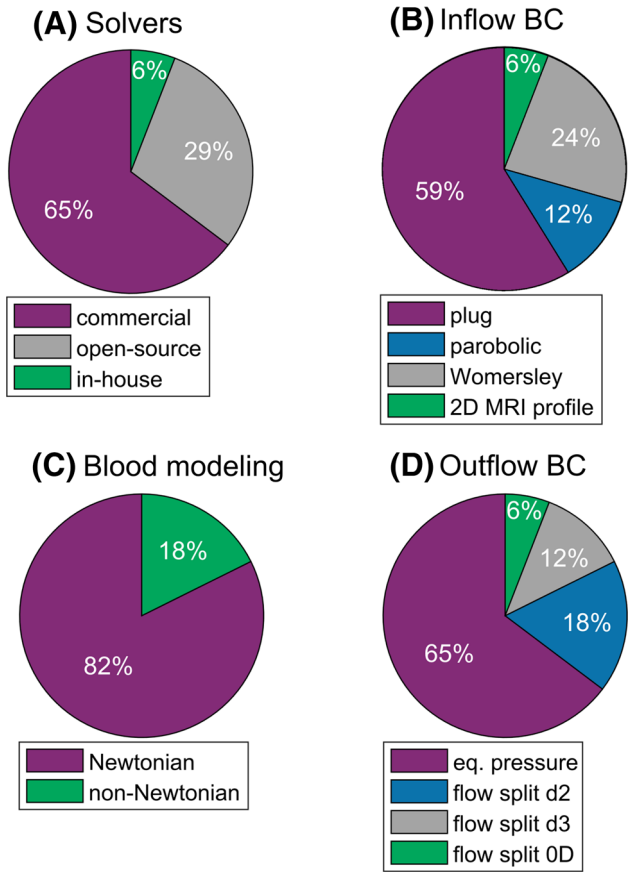


**Fig. 2** Distribution of methodological details regarding the variability of hemodynamic simulations: **a** type of the fluid flow solver, **b** type of inflow boundary condition (BC), **c** concept of blood treatment, **d** type of outflow boundary condition (d2 and d3 relate to the power coefficient of Murray's law, 0D indicated the application of a reduced splitting model)

groups), or the cube of the corresponding vessel diameter (two groups) [20].

Finally, all groups assumed rigid vessel wall conditions and no participant carried out fluid–structure interaction simulations to account for vessel movement or occurring wall stresses.

### Blood modeling

The treatment of blood with respect to its material properties was relatively consistent among the groups. Since blood is an incompressible fluid, the assumption of a constant density is well-accepted and values ranging between 1000 and 1100 kg/m$^3$ were applied (median = 1056 kg/m$^3$).

Regarding the choice of viscosity, no clear consensus exists. While some studies claim that non-Newtonian effects influence the simulation results [21, 22], others have found no significant impact of available models on the flow fields [23, 24]. Nevertheless, researchers agree that the choice of blood treatment has rather secondary effects compared to primary influences, e.g., geometry and inflow conditions. Within MATCH, 14 groups (82%) assumed a Newtonian fluid with a mean dynamic viscosity of $3.65 \pm 0.21$ mPa s. The remaining three groups applied non-Newtonian models (either power law models or the *Carreau* model).

## Results

As a summary of the challenge, Table 1 contains the group-specific settings for their numerical investigation as well as their choice regarding the ruptured aneurysm.

### Rupture risk assessment

In the context of MATCH, the assessment of aneurysm rupture risk was mostly carried out using morphological in combination with hemodynamics parameters. For instance, only four groups considered patient information such as the aneurysm site. In this regard, it must be noted that only the DICOM dataset was provided to the participants to assess the ability of biomedical engineering related analysis. Hence, clinically relevant factors such as age, sex, smoking, hypertension were not disclosed.

Only three morphological parameters were chosen more than once (aspect ratio, size ratio and undulation index), while the following parameters were chosen only once: aneurysm neck area, aneurysm width, height-to-width ratio, bulge location, parent vessel diameter, volume-to-ostium ratio, non-sphericity index, aneurysm surface curvature, ratio between each aneurysm's volume, and volume of each aneurysm's least bounding sphere.

Besides the morphological analyses, participants applied hemodynamics parameters to assess the rupture probability of each aneurysm. By far the most often used parameter was WSS (in different variants), which was calculated by 13 groups. The second most applied variable was the oscillatory shear index (OSI, 9) followed by pressure (5), maximum velocity, velocity fluctuation, and relative residence time (each 2). The following parameters were used only once: inflow concentration index, energy loss, vorticity, helicity, low shear area, kinetic energy, and spectral power index.

Table 2 contains the rupture risk assessment strategies of all participants and reveals the basis for the individual decisions. Furthermore, it provides an overview of the usage of morphological and hemodynamic parameters by each group. One should notice that only five groups applied hemodynamic parameters exclusively to assess the rupture probability.

**Table 2** Overview of the participants rupture risk assessment strategies containing the number of considered morphologic as well as hemodynamic parameters (correct choices are highlighted as bold)

| Group | Rupture risk assessment strategy | Parameters | |
|---|---|---|---|
| | | Morph | Hemo |
| **1** | **Logistic regression models (based on CFD simulations of 1920 aneurysms)** [7] | **9** | **7** |
| 2 | Rupture resemblance score (based on CFD simulations of 542 aneurysms) [25] | 2 | 2 |
| 3 | Aneurysm size and energy loss [26] | 1 | 1 |
| 4 | WSS difference between the maximum and minimum flow condition | 0 | 1 |
| 5 | Combination of size, irregularity, low aspect ratio and low WSS, high OSI, high-frequency WSS instabilities [27] | 3 | 3 |
| **6** | **Location, diameter, WSS** | **2** | **1** |
| 7 | Location, size, ratio of volume and volume of least bounding sphere, streamlines, and WSS | 3 | 1 |
| **8** | **Internal scoring system based on dome/neck ratio, blebs, TAWSS, change in instantaneous WSS, OSI on daughter blebs** | **2** | **3** |
| 9 | Visual inspection of morphology (non-spherical shape) and flow instability (turbulent-like flow) | 1 | 1 |
| 10 | Pressure and WSS ratios | 0 | 2 |
| 11 | Size and low WSS | 1 | 1 |
| 12 | WSS, TAWSS, OSI | 0 | 3 |
| 13 | Rupture resemblance score (based on CFD simulations of 542 aneurysms) [25] | 1 | 2 |
| 14 | Aspect ratio, pressure difference, OSI, rupture risk parameter based on WSS and averaged velocity | 1 | 4 |
| **15** | **TAWSS, OSI, RRT, pressure distribution, stagnation points** | **0** | **5** |
| 16 | Relative changes of WSS, velocity, pressure, vorticity, helicity | 0 | 5 |
| 17 | Size, aspect ratio, WSS, OSI, RRT, ICI | 2 | 4 |

With *(TA)WSS* (time-averaged) wall shear stress, *OSI* oscillatory shear index, *RRT* relative residence time, *ICI* inflow concentration index

## Selections by the challenge participants

Participating groups selected the following aneurysms as being the ruptured one: Most groups (7/41%) selected aneurysm A as the most probable candidate, which is the largest one. It can be observed that five of these groups used low WSS in combination with increased OSI as indicators for aneurysm rupture.

Four groups (24%) correctly selected aneurysm E as being the ruptured one. While one group combined clinically relevant information (e.g., aneurysm site) with simulation results, two groups applied rupture risk assessment models. These include multiple morphological as well as hemodynamic parameters that were associated with rupture in previous studies. Furthermore, it must be mentioned that one of the successful groups, focusing on hemodynamics exclusively, analyzed not only surface parameters, but also the flow behavior within the aneurysm (e.g., inflow jet, presence of multiple vortices).

Aneurysms C and D were selected by three groups each (18%). The selections by these groups were based on single hemodynamic parameters or visual inspection of morphology and flow instability. Finally, no group selected aneurysm B, which was the smallest one.

The rupture probability ranking revealed that aneurysm E was correctly selected by four groups (23.5%). Furthermore, the rupture probability of aneurysm E was ranked second by three groups (17.5%), third by four groups (23.5%), and fourth by two groups (12%). Finally, another four groups (23.5%) judged aneurysm E as being the least prone to rupture. Thus, a strong variability regarding the calculated rupture probability of the actual ruptured aneurysm exists. Table 3 contains the rupture risk probability rankings of all groups.

**Table 3** Rupture probability ranking provided by each MATCH participant based on the individual segmentations and hemodynamic simulations

| Group | Rupture probability ranking | | | | |
|---|---|---|---|---|---|
| | 1st | 2nd | 3rd | 4th | 5th |
| 1 | **E** | D | A | C | B |
| 2 | A | C | D | **E** | B |
| 3 | C | D | **E** | B | A |
| 4 | D | **E** | A | B | C |
| 5 | A | **E** | C | D | B |
| 6 | **E** | A | C | D | B |
| 7 | A | **E** | C | D | B |
| 8 | **E** | C | D | A | B |
| 9 | D | C | A | **E** | B |
| 10 | D | A | **E** | C | B |
| 11 | A | C | **E** | D | B |
| 12 | C | B | D | A | **E** |
| 13 | C | A | D | B | **E** |
| 14 | A | C | D | B | **E** |
| 15 | **E** | D | C | A | B |
| 16 | C | A | B | D | **E** |
| 17 | A | C | **E** | D | B |

The ruptured aneurysm (E) is highlighted in bold. Notice the strong variability with an exception for the smallest aneurysm B as being the least endangered

## Discussion

MATCH focused on the comparison of segmentation and simulation algorithms to assess the rupture risk probability of IAs. While it was demonstrated in the first phase that clear variations regarding the aneurysm surface representation exist [17], the second phase presents the real-world variability of rupture risk assessment.

### The role of hemodynamic simulations

It can be observed in the literature that an increasing number of blood flow simulations is being performed to improve the knowledge on patient-individual flow characteristics of IAs. While some studies focused on detailed hemodynamic descriptions for a limited number of cases [28, 29], others investigated blood flow variables in larger cohorts [4, 30, 31]. In this regard, significant differences between unruptured and ruptured IAs were identified. However, only snapshots of the disease state are considered and longitudinal studies are in a clear minority [32, 33].

In the frame of the second MATCH phase, it was observed that most groups applied not only hemodynamic, but also morphological parameters for their evaluation of the rupture probability (Table 2). This emphasizes the fact that at least with regard to the present knowledge, flow simulations cannot provide all necessary information to reliably assess IA rupture risk. Instead, a multivariate analysis by combining clinically relevant metadata with advanced morphological and hemodynamic quantification appears to be more promising.

Additionally, it is important to mention that certain minimum requirements with respect to the simulation setup are needed in the future to ensure plausible numerical results. These include appropriate segmentations, the generation of a sufficient volume mesh, the choice of justifiable boundary conditions, the selection of a verified fluid flow solver and a realistic modeling of blood. Apart from the first criterion, which has primary impact on the simulation results, no strong variations were present among the participating groups. However, clear differences regarding the subsequent data evaluation occurred as described in the following section.

### Rupture risk assessment

In contrast to earlier aneurysm challenges, which predefined the simulation domains or boundary conditions [13, 15], MATCH was designed to give all participants the chance to completely apply their own strategies. A realistic scenario was created, in which researchers were confronted with clinical image data and aneurysm risk quantification is requested by the attending physicians. In this regard, it was noted that groups created individualized workflows to obtain segmentation and simulation results. Furthermore, the subsequent analyses revealed clear differences with respect to extent. While some groups only applied one or two parameters, other included up to sixteen in well-trained models. Specifically, several groups used low WSS in combination with high OSI to identify the ruptured aneurysm (e.g., all successful groups). However, aneurysm rupture does not necessarily take place in regions of lowest WSS and highest OSI, respectively [14]. Additionally, the sophisticated, model-based selections were related to strong clinical, as well as bioengineering experience. These models include either multiple morphological and hemodynamic parameters as well as the aneurysm's location [7], or advanced scoring systems with a particular focus on blebs and flow features.

Future studies require a systematic uncertainty quantification to assess the robustness of the applied models. In this regard, initial investigations in the context of MATCH are carried out [34] and existing examples from cardiovascular research could be transferred to cerebrovascular questions [35–37].

### Recommendations

The investigation of five IAs in a single patient certainly does not enable the derivation of generalizable rules regarding the future assessment of aneurysm rupture probabilities. However, certain recommendations can be formulated, which arise from observations during this international challenge:

1. MATCH emphasizes the importance of appropriate segmentation and should motivate groups to put highest efforts in this presimulation step. It was shown that one group, which reconstructed the neck of the ruptured aneurysm with the highest accuracy in MATCH Phase I [17], was also among the successful groups in Phase II. Further, the other three successful groups submitted no outlying segmentation results.
2. To obtain plausible blood flow results, a minimum spatial resolution of the discretized domain is needed to avoid influences due to mesh-dependence (e.g., most groups applied a base size of approximately 0.1 mm).
3. Since none of the groups that assumed steady-state flow conditions chose the correct aneurysm, time-dependent blood flow simulation should be carried out. This enables the prediction of complex transient flow phenomena, which were associated with rupture [38–40]. Further, as computational resources continue to improve, simulation times should not be a problem in the future. Nevertheless, as presented in Table 1, the type of inflow condition as well as the choice of blood description appear to be rather of secondary importance [16].

4. Regarding the outlet boundary condition, it is well known that with an increasing number of outflow cross sections, the influence on the flow fields rises. Thus, although the majority of groups used constant pressure conditions, it should be avoided by applying advanced flow-splitting methods. Furthermore, additional quantification studies are required in order to be able to simulate larger domains of the cerebral vasculature.
5. To identify relevant rupture risk assessment parameters in the future, they must be consistently compared in future studies. Within the challenge, neither single nor few morphological and hemodynamic parameters alone were sufficient for a robust and reliable rupture risk evaluation of IAs. Instead, the application of advanced and validated prediction models was successful, which include a variety of independent factors [7]. These consist of clinically important information from the patient as well as individual shape and flow parameters.

## Limitations

It must be noted that certain limitations exist regarding this challenge. First, only one patient was included in this study, although harboring five aneurysms. Thus, no generalizable conclusions are possible, and investigations with an increased number of cases are desirable. However, the inclusion of more cases would likely have led to a decreased number of participants and therefore to a limited comparability among real-world approaches.

Second, since no patient-specific wall information was provided in the frame of the study, all hemodynamic simulations were carried out based on the assumption of rigid vessels. Hence, the role of aneurysm vessel walls regarding aneurysm rupture remains unclear. Nevertheless, if reliable and accurate wall information is available, it is recommended to include it in future studies [41, 42].

Third, due to a lack of measured data, no patient-specific boundary conditions were provided. This, however, is a common situation in clinical practice. Especially in patients with SAH, flow measurements would mean an additional examination, which is inappropriate in emergency situations. In addition, such a measurement would not necessarily reflect the hemodynamic situation that was present during the rupture. In patients with innocent aneurysms, patient-specific flow conditions can be determined more easily, but even then, it would only be a snapshot in a physical state of rest that cannot reflect the fluctuations caused by different daily activities.

Fourth, the experience of each participant was not queried, as was done in previous challenges [16]. On the one hand, it certainly would have been interesting to correlate experience with rupture risk assessment outcome. However, "experience" is difficult to measure since neither the (active or passive) duration nor the number of simulated cases is an objective metric. Furthermore, multiple disciplines come into play (e.g., biomedical engineers, physicians, computer scientists), with personnel who possess different backgrounds and skills. Also, verified and validated techniques should be successful even with minor experience. Therefore, the challenge organizers decided against the inclusion of experience into the study.

Finally, it should be stated that MATCH was not designed to determine whether or not CFD is able to predict aneurysm rupture in general. It should rather be seen as an instrument that reveals potentials but also limitations of existing methods that include hemodynamics, but also emphasizes where further improvements are required toward clinical support. Hence, from the perspective of the challenge organizers, the aim of the study was not to end up with as many successful predictions as possible. Rather, the real value becomes visible in the separation between successful and unsuccessful choices and the associated methodologies. Therefore, MATCH should encourage groups with correct predictions to further improve their models and communicate them accordingly. Additionally, groups with incorrect aneurysm selection can re-evaluate their workflows for image-based blood flow simulations and integrate more advanced techniques to improve their methods.

## Conclusions

To demonstrate and compare existing blood flow simulation techniques for the rupture risk assessment of IAs, an international challenge was announced. Participants were given 3D imaging data containing five intracranial aneurysms from one patient and were asked to assess which aneurysm ruptured. Overall, 17 groups from 11 countries participated, and 4 groups correctly identified the ruptured aneurysm. Although this is only a 24% group success rate, successful selections were based on clinical data as well as advanced probability models. Thus, the challenge highlights the importance of multivariate analyses that combine clinically relevant metadata with advanced morphological and hemodynamic quantification. Furthermore, it is essential to work together to drive consensus on approach and best practices for hemodynamics simulations.

**Acknowledgements** This study was funded by the Federal Ministry of Education and Research in Germany within the Forschungscampus *STIMULATE* (Grant Number 13GW0095A) and the German Research Foundation (Grant Number 399581926). The authors highly acknowledge participants of MATCH Phase I, who contributed their segmentation results.

## Compliance with ethical standards

**Conflict of interest** The authors declare they have no conflict of interest.

**Ethical approval** All procedures performed in studies involving human participants were in accordance with the ethical standards of the institutional and/or national research committee and with the 1964 Helsinki Declaration and its later amendments or comparable ethical standards.

**Informed consent** Informed consent was obtained from all individual participants included in the study.

## References


1. Steinman DA, Milner JS, Norley CJ, Lownie SP, Holdsworth DW (2003) Image-based computational simulation of flow dynamics in a giant intracranial aneurysm. AJNR Am J Neuroradiol 24(4):559–566
2. Kobayashi N, Miyachi S, Okamoto T, Hattori K, Kojima T, Nakai K, Qian S, Takeda H, Yoshida J (2004) Computer simulation of flow dynamics in an intracranial aneurysm. Effects of vessel wall pulsation on a case of ophthalmic aneurysm. Interv Neuroradiol: J Peritherapeutic Neuroradiol Surg Proced Relat Neurosci 10(Suppl 1):155–160. https://doi.org/10.1177/15910199040100s127
3. Xiang J, Natarajan SK, Tremmel M, Ma D, Mocco J, Hopkins LN, Siddiqui AH, Levy EI, Meng H (2011) Hemodynamic-morphologic discriminants for intracranial aneurysm rupture. Stroke 42(1):144–152. https://doi.org/10.1161/STROKEAHA.110.592923
4. Xiang J, Yu J, Snyder KV, Levy EI, Siddiqui AH, Meng H (2016) Hemodynamic-morphological discriminant models for intracranial aneurysm rupture remain stable with increasing sample size. J Neurointerv Surg 8(1):104–110. https://doi.org/10.1136/neurintsurg-2014-011477
5. Cebral JR, Mut F, Weir J, Putman C (2011) Quantitative characterization of the hemodynamic environment in ruptured and unruptured brain aneurysms. AJNR Am J Neuroradiol 32(1):145–151. https://doi.org/10.3174/ajnr.A2419
6. Cebral JR, Mut F, Weir J, Putman CM (2011) Association of hemodynamic characteristics and cerebral aneurysm rupture. AJNR Am J Neuroradiol 32(2):264–270. https://doi.org/10.3174/ajnr.A2274
7. Detmer FJ, Chung BJ, Mut F, Slawski M, Hamzei-Sichani F, Putman C, Jiménez C, Cebral JR (2018) Development and internal validation of an aneurysm rupture probability model based on patient characteristics and aneurysm location, morphology, and hemodynamics. Int J Comput Assist Radiol Surg 13(11):1767–1779. https://doi.org/10.1007/s11548-018-1837-0
8. Berg P, Stucht D, Janiga G, Beuing O, Speck O, Thévenin D (2014) Cerebral blood flow in a healthy Circle of Willis and two intracranial aneurysms: computational fluid dynamics versus four-dimensional phase-contrast magnetic resonance imaging. J Biomech Eng. https://doi.org/10.1115/1.4026108
9. Roloff C, Stucht D, Beuing O, Berg P (2019) Comparison of intracranial aneurysm flow quantification techniques: standard PIV vs stereoscopic PIV vs tomographic PIV vs phase-contrast MRI vs CFD. J Neurointerv Surg 11(3):275–282. https://doi.org/10.1136/neurintsurg-2018-013921
10. Raschi M, Mut F, Byrne G, Putman CM, Tateshima S, Viñuela F, Tanoue T, Tanishita K, Cebral JR (2012) CFD and PIV analysis of hemodynamics in a growing intracranial aneurysm. Int J Numer Methods Biomed Eng 28(2):214–228. https://doi.org/10.1002/cnm.1459
11. Paliwal N, Damiano RJ, Varble NA, Tutino VM, Dou Z, Siddiqui AH, Meng H (2017) Methodology for computational fluid dynamic validation for medical use: application to intracranial aneurysm. J Biomech Eng. https://doi.org/10.1115/1.4037792
12. Bouillot P, Brina O, Ouared R, Lovblad K-O, Farhat M, Pereira VM (2014) Particle imaging velocimetry evaluation of intracranial stents in sidewall aneurysm: hemodynamic transition related to the stent design. PLoS ONE 9(12):e113762. https://doi.org/10.1371/journal.pone.0113762
13. Steinman DA, Hoi Y, Fahy P, Morris L, Walsh MT, Aristokleous N, Anayiotos AS, Papaharilaou Y, Arzani A, Shadden SC, Berg P, Janiga G, Bols J, Segers P, Bressloff NW, Cibis M, Gijsen FH, Cito S, Pallarés J, Browne LD, Costelloe JA, Lynch AG, Degroote J, Vierendeels J, Fu W, Qiao A, Hodis S, Kallmes DF, Kalsi H, Long Q, Kheyfets VO, Finol EA, Kono K, Malek AM, Lauric A, Menon PG, Pekkan K, Esmaily Moghadam M, Marsden AL, Oshima M, Katagiri K, Peiffer V, Mohamied Y, Sherwin SJ, Schaller J, Goubergrits L, Usera G, Mendina M, Valen-Sendstad K, Habets DF, Xiang J, Meng H, Yu Y, Karniadakis GE, Shaffer N, Loth F (2013) Variability of computational fluid dynamics solutions for pressure and flow in a giant aneurysm: the ASME 2012 summer bioengineering conference CFD challenge. J Biomech Eng 135(2):21016. https://doi.org/10.1115/1.4023382
14. Janiga G, Berg P, Sugiyama S, Kono K, Steinman DA (2015) The computational fluid dynamics rupture challenge 2013—phase I: prediction of rupture status in intracranial aneurysms. AJNR Am J Neuroradiol 36(3):530–536. https://doi.org/10.3174/ajnr.A4157
15. Berg P, Roloff C, Beuing O, Voss S, Sugiyama S-I, Aristokleous N, Anayiotos AS, Ashton N, Revell A, Bressloff NW, Brown AG, Chung BJ, Cebral JR, Copelli G, Fu W, Qiao A, Geers AJ, Hodis S, Dragomir-Daescu D, Nordahl E, Bora Suzen Y, Owais Khan M, Valen-Sendstad K, Kono K, Menon PG, Albal PG, Mierka O, Münster R, Morales HG, Bonnefous O, Osman J, Goubergrits L, Pallares J, Cito S, Passalacqua A, Piskin S, Pekkan K, Ramalho S, Marques N, Sanchi S, Schumacher KR, Sturgeon J, Švihlová H, Hron J, Usera G, Mendina M, Xiang J, Meng H, Steinman DA, Janiga G (2015) The computational fluid dynamics rupture challenge 2013–phase II: variability of hemodynamic simulations in two intracranial aneurysms. J Biomech Eng 137(12):121008. https://doi.org/10.1115/1.4031794
16. Valen-Sendstad K, Bergersen AW, Shimogonya Y, Goubergrits L, Bruening J, Pallares J, Cito S, Piskin S, Pekkan K, Geers AJ, Larrabide I, Rapaka S, Mihalef V, Fu W, Qiao A, Jain K, Roller S, Mardal K-A, Kamakoti R, Spirka T, Ashton N, Revell A, Aristokleous N, Houston JG, Tsuji M, Ishida F, Menon PG, Browne LD, Broderick S, Shojima M, Koizumi S, Barbour M, Aliseda A, Morales HG, Lefèvre T, Hodis S, Al-Smadi YM, Tran JS, Marsden AL, Vaippummadhom S, Einstein GA, Brown AG, Debus K, Niizuma K, Rashad S, Sugiyama S-I, Owais Khan M, Updegrove AR, Shadden SC, Cornelissen BMW, Majoie CBLM, Berg P, Saalfield S, Kono K, Steinman DA (2018) Real-world variability in the prediction of intracranial aneurysm wall shear stress. The 2015 international aneurysm CFD challenge. Cardiovasc Eng Tech 9(4):544–564. https://doi.org/10.1007/s13239-018-00374-2
17. Berg P, Voß S, Saalfeld S, Janiga G, Bergersen AW, Valen-Sendstad K, Bruening J, Goubergrits L, Spuler A, Cancelliere NM, Steinman DA, Pereira VM, Chiu TL, Tsang ACO, Chung BJ, Cebral JR, Cito S, Pallarès J, Copelli G, Csippa B, Paál G, Fujimura S, Takao H, Hodis S, Hille G, Karmonik C, Elias S, Kellermann K, Khan MO, Marsden AL, Morales HG, Piskin S, Finol EA, Pravdivtseva M, Rajabzadeh-Oghaz H, Paliwal N, Meng H, Seshadhri S, Howard M, Shojima M, Sugiyama S-I, Niizuma K, Sindeev S, Frolov S, Wagner T, Brawanski A, Qian Y, Wu Y-A, Carlson KD, Dragomir-Daescu D, Beuing O (2018) Multiple Aneurysms AnaTomy CHallenge 2018 (MATCH): phase I: segmentation. Car-

diovas Eng Technol 9(4):565–581. https://doi.org/10.1007/s13239-018-00376-0
18. Berg P, Saalfeld S, Voß S, Redel T, Preim B, Janiga G, Beuing O (2018) Does the DSA reconstruction kernel affect hemodynamic predictions in intracranial aneurysms? An analysis of geometry and blood flow variations. J Neurointerv Surg 10(3):290–296. https://doi.org/10.1136/neurintsurg-2017-012996
19. Chnafa C, Brina O, Pereira VM, Steinman DA (2018) Better than nothing: a rational approach for minimizing the impact of outflow strategy on cerebrovascular simulations. AJNR Am J Neuroradiol 39(2):337–343. https://doi.org/10.3174/ajnr.A5484
20. Murray CD (1926) The physiological principle of minimum work: I. The vascular system and the cost of blood volume. In: Proceedings of the national academy of sciences of the United States of America 12(3):207–214
21. Carty G, Chatpun S, Espino DM (2016) Modeling blood flow through intracranial aneurysms. a comparison of newtonian and non-newtonian viscosity. J Med Biol Eng 36(3):396–409. https://doi.org/10.1007/s40846-016-0142-z
22. Frolov S, Sindeev S, Liepsch D, Balasso A, Arnold P, Kirschke JS, Prothmann S, Potlov AY (2018) Newtonian and non-Newtonian blood flow at a 90o-birfurcation of the cerebral artery. A comparative study of fluid viscosity models. J Mech Med Biol 18(05):1850043. https://doi.org/10.1142/s0219519418500434
23. Fisher C, Rossmann JS (2009) Effect of non-newtonian behavior on hemodynamics of cerebral aneurysms. J Biomech Eng 131(9):91004. https://doi.org/10.1115/1.3148470
24. Morales HG, Larrabide I, Geers AJ, Aguilar ML, Frangi AF (2013) Newtonian and non-Newtonian blood flow in coiled cerebral aneurysms. J Biomech 46(13):2158–2164. https://doi.org/10.1016/j.jbiomech.2013.06.034
25. Xiang J, Yu J, Choi H, Dolan Fox JM, Snyder KV, Levy EI, Siddiqui AH, Meng H (2015) Rupture Resemblance Score (RRS): toward risk stratification of unruptured intracranial aneurysms using hemodynamic-morphological discriminants. J Neurointerv Surg 7(7):490–495. https://doi.org/10.1136/neurintsurg-2014-011218
26. Qian Y, Takao H, Umezu M, Murayama Y (2011) Risk analysis of unruptured aneurysms using computational fluid dynamics technology: preliminary results. AJNR Am J Neuroradiol 32(10):1948–1955. https://doi.org/10.3174/ajnr.A2655
27. Khan MO, Chnafa C, Gallo D, Molinari F, Morbiducci U, Steinman DA, Valen-Sendstad K (2017) On the quantification and visualization of transient periodic instabilities in pulsatile flows. J Biomech 52:179–182. https://doi.org/10.1016/j.jbiomech.2016.12.037
28. Valen-Sendstad K, Piccinelli M, Steinman DA (2014) High-resolution computational fluid dynamics detects flow instabilities in the carotid siphon: implications for aneurysm initiation and rupture? J Biomech 47(12):3210–3216. https://doi.org/10.1016/j.jbiomech.2014.04.018
29. Valen-Sendstad K, Steinman DA (2014) Mind the gap: impact of computational fluid dynamics solution strategy on prediction of intracranial aneurysm hemodynamics and rupture status indicators. AJNR Am J Neuroradiol 35(3):536–543. https://doi.org/10.3174/ajnr.A3793
30. Chung BJ, Doddasomayajula R, Mut F, Detmer F, Pritz MB, Hamzei-Sichani F, Brinjikji W, Kallmes DF, Jimenez CM, Putman CM, Cebral JR (2017) Angioarchitectures and Hemodynamic Characteristics of Posterior Communicating Artery Aneurysms and Their Association with Rupture Status. AJNR Am J Neuroradiol 38(11):2111–2118. https://doi.org/10.3174/ajnr.A5358
31. Detmer FJ, Chung BJ, Mut F, Pritz M, Slawski M, Hamzei-Sichani F, Kallmes D, Putman C, Jimenez C, Cebral JR (2018) Development of a statistical model for discrimination of rupture status in posterior communicating artery aneurysms. Acta Neurochirur 160(8):1643–1652. https://doi.org/10.1007/s00701-018-3595-8
32. Boussel L, Rayz V, McCulloch C, Martin A, Acevedo-Bolton G, Lawton M, Higashida R, Smith WS, Young WL, Saloner D (2008) Aneurysm growth occurs at region of low wall shear stress: patient-specific correlation of hemodynamics and growth in a longitudinal study. Stroke 39(11):2997–3002. https://doi.org/10.1161/STROKEAHA.108.521617
33. Soize S, Gawlitza M, Raoult H, Pierot L (2016) Imaging follow-up of intracranial aneurysms treated by endovascular means: Why, When, and How? Stroke 47(5):1407–1412. https://doi.org/10.1161/STROKEAHA.115.011414
34. Goubergrits L, Hellmeier F, Bruening J, Spuler A, Hege HC, Voß S, Janiga G, Saalfeld S, Beuing O, Berg P (2019) Multiple Aneurysms AnaTomy CHallenge 2018 (MATCH)—Uncertainty quantification of geometric rupture risk parameters. BioMed Eng OnLine 18(1):35. https://doi.org/10.1186/s12938-019-0657-y
35. Mirams GR, Pathmanathan P, Gray RA, Challenor P, Clayton RH (2016) Uncertainty and variability in computational and mathematical models of cardiac physiology. J Physiol 594(23):6833–6847. https://doi.org/10.1113/JP271671
36. Sankaran S, Kim HJ, Choi G, Taylor CA (2016) Uncertainty quantification in coronary blood flow simulations: impact of geometry, boundary conditions and blood viscosity. J Biomech 49(12):2540–2547. https://doi.org/10.1016/j.jbiomech.2016.01.002
37. Schiavazzi DE, Arbia G, Baker C, Hlavacek AM, Hsia TY, Marsden AL, Vignon-Clementel IE (2016) Uncertainty quantification in virtual surgery hemodynamics predictions for single ventricle palliation. Int J Numer Methods Biomed Eng 32(3):e02737. https://doi.org/10.1002/cnm.2737
38. Doddasomayajula R, Chung B, Hamzei-Sichani F, Putman CM, Cebral JR (2017) Differences in hemodynamics and rupture rate of aneurysms at the bifurcation of the basilar and internal carotid arteries. AJNR Am J Neuroradiol 38(3):570–576. https://doi.org/10.3174/ajnr.A5088
39. Sano T, Ishida F, Tsuji M, Furukawa K, Shimosaka S, Suzuki H (2017) Hemodynamic differences between ruptured and unruptured cerebral aneurysms simultaneously existing in the same location: 2 case reports and proposal of a novel parameter oscillatory velocity index. World Neurosurg 98:868.e5–868.e10. https://doi.org/10.1016/j.wneu.2016.12.047
40. Berg P, Beuing O (2018) Multiple intracranial aneurysms: a direct hemodynamic comparison between ruptured and unruptured vessel malformations. Int J Comput Assist Radiol Surg 13(1):83–93. https://doi.org/10.1007/s11548-017-1643-0
41. Voß S, Glaßer S, Hoffmann T, Beuing O, Weigand S, Jachau K, Preim B, Thévenin D, Janiga G, Berg P (2016) Fluid-structure simulations of a ruptured intracranial aneurysm: constant versus patient-specific wall thickness. Comput Math Methods Med 2016:9854539. https://doi.org/10.1155/2016/9854539
42. Cebral J, Ollikainen E, Chung BJ, Mut F, Sippola V, Jahromi BR, Tulamo R, Hernesniemi J, Niemelä M, Robertson A, Frösen J (2017) Flow conditions in the intracranial aneurysm lumen are associated with inflammation and degenerative changes of the aneurysm wall. AJNR Am J Neuroradiol 38(1):119–126. https://doi.org/10.3174/ajnr.A4951